Assessing the Impacts of Power Outage on Community Overheating Risk during Extreme Heat Waves

Luis Rodriguez-Garcia
The University of Utah
luis.rodriguez@utah.edu

Miguel Heleno
Lawrence Berkeley National Laboratory
miguelheleno@lbl.gov

Masood Parvania
The University of Utah
masood.parvania@utah.edu

Abstract

Communities worldwide are experiencing more frequent and intense heat waves, where the increased use of energy-intensive cooling systems is putting additional pressure on the power system. While power utility companies reduce this overload by applying controlled outages, this disruption inequitably impacts communities dependent on the electricity supply to unbearable indoor temperatures during extreme weather. To assess the relationship between power outages and overheating risk, this paper formulates a framework to evaluate the community overheating risk when exposed to rotating outages during heat waves. The framework is based on a set of metrics that initially evaluates the overheating risk at a household level, which is aggregated to the power distribution system nodes and then scored to quantify the overall feeder overheating inequity based on a thermal simulation of the indoor temperature when a power outage occurs during a heat wave. A sensitivity analysis is also conducted to assess the impact of distributed energy resources on the community vulnerability and overheating risk inequity. The proposed framework is tested on the IEEE 33-node test system, where it succeeds in identifying highly vulnerable areas where planning and operational decisions may enhance community resilience to heat waves.

1. Introduction

1.1. Background and Literature Review

Climate change has increased the frequency and intensity of heat waves, which represent one of the extreme weather events that causes most deaths worldwide, with more than 70,000 deaths during the 2003 European heat wave, and hundreds of excess death occurring in the US during 2021 Northwest and Canada heat wave [1]. To avoid the risk of heat-related illness during heat waves, communities are forced to ramp up the use of cooling systems at their households, e.g., heating-ventilation-air conditioning (HVAC) systems, to mitigate thermal discomfort and risk, which cause overloading on the power distribution systems. In addition, heat waves compromise the ability of Independent System Operators to ensure generation-demand balance, as high temperatures also limit the operation of thermal generation units, and reduce the efficiency and power transfer capability of the transmission system, as occurred recently during the 2020 California heat wave [2].

In a scenario where the generation and demand imbalance can trigger a large-scale blackout, the independent system operators encourage power distribution system operators to schedule rotating outages, where feeders are alternately disconnected to reduce the loading at power substations. These controlled power outages, occurring during an ongoing heat wave, expose customers to increased indoor temperatures due to non-operative HVAC systems; however, the effects of high temperature are not equally distributed among all the community members affected by the power outage [3]. Disadvantaged communities and population of heat-sensitive groups are commonly located in underserved areas, where access to distributed energy resources (DERs) is limited compared to higher income neighborhoods, increasing the chances of extended power interruptions. In addition, the houses associated with these groups are commonly identified for having poor insulation, as well as antiquated and low efficient appliances causing high energy cost and intensifying their overheating risk [4].

URI: https://hdl.handle.net/10125/106734
978-0-9981331-7-1

Power distribution system resilience to extreme weather events can be quantified and enhanced using different approaches, e.g., [5], [6]. The literature includes metrics to quantify the impacts of automation in power distribution system resilience to extreme weather [7], and metrics to quantify the interdependence between the resilience of power and water distribution systems [8]. Enhancing the resilience and mitigating inequity induced by outages during extreme heat, on the other hand, requires indicators that measure the impact of power outages during heat waves, which are intended to provide sensitivity to make planning decisions by power utility companies and for policymakers to define guidelines tackling heat inequity.

The impacts of power outage during heat waves on the resilience of buildings and community risk has been discussed in literature from the household standpoint. A framework on resilience of buildings during extreme weather events and power outages is presented in [9]. Multiple metrics have been defined to determine the thermal comfort and overheating risk, many of these based on international standards (e.g., IEC, ISO) [10]. In [11], an assessment to determine the duration of rotating outages, and also, the impact of notifying customers as a method to mitigate the impact of the heat wave during the outage. In [12], an assessment of the impact of power outages in a assisted living facility during heat waves is considered, where the benefits of passive measure are evaluated. An assessment on the benefits of pre-cooling as an strategy to mitigate overheating risk during heat waves is presented in [13]. An evaluation of the resilience of buildings after implementing passive solutions when exposed to heat waves in grid-on and grid-off scenarios is presented in [4].

While multiple metrics have been developed to determine the thermal comfort and overheating risk at a household level, a research gap exists when linking the overheating risk to the power distribution system. More specifically, the existing approaches fail to capture the locational overheating risk among the power distribution system nodes when affected by a power outage, which consequently fail to provide insights into the overheating inequity experienced by customers at different locations.

1.2. Contribution and Paper Structure

This paper proposes a framework to quantify the community overheating risk and inequity to power outages during heat waves, which is summarized in Fig. 1. In this three-stage framework, a house thermal simulation is first implemented to estimate the indoor air temperature at the house, given the outdoor air temperature, the thermal attributes and cooling system characteristics of the house, and the power availability given the outage location and duration. Based on the temperature estimation obtained in the house thermal simulation, a set of metrics are evaluated to assess the overheating risk and inequity that a community is exposed during a power outage. The metrics initially assess the overheating risk at a household level, which is then aggregated to the power distribution system nodes to determine the overheating risk spatial distribution through the power network. Then, the overheating risk inequity is quantified at the feeder level based on the spatial distribution of the overheating risk. The developed thermal simulation combined with the risk and inequity metrics provide a tool for the implementation of sensitivity analyses to evaluate the impact including automation and DER installation.

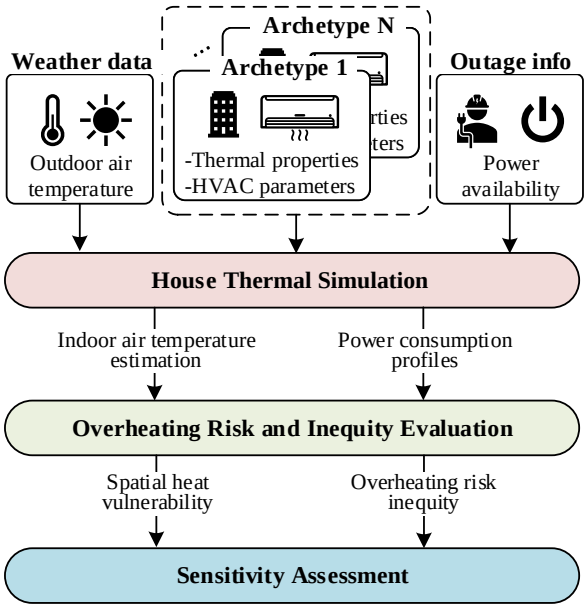

Figure 1. Framework to evaluate overheating risk and inequity during power outages

The remainder of the paper is divided as follows: Section 2 discusses the impacts of power outages in the overheating risk and inequity during heat waves. Section 3 details the developed framework for the outage-induced overheating risk and inequity assessment. Results are presented and discussed in Section 4 and conclusions are drawn in Section 5.

2. Overheating Risk during Power Outages: Exposure and Inequity

The increased temperatures caused by extreme heat in cities expose disadvantaged communities—communities suffering from a

combination of economic, environmental, and health burdens [14]—to *overheating risk* when subject to unsafe temperatures during long periods, potentially experiencing discomfort or even heat-related illnesses [15]. While the HVAC system utilization mitigates the risk of overheating, the increased electricity consumption during the heat wave peak may force power utilities to apply rotating outages, where groups of feeders are alternatively disconnected for short periods to reduce the total loading at power substations during the emergency period. However, these power outages expose customers to quick increments of the indoor air temperature due to the outage of cooling systems, increasing the overheating risk for the individuals residing in this location.

The overheating risk resulting from a power outage during a heat wave is illustrated in Fig. 2. Suppose that the indoor air temperature is initially fixed in a temperature setpoint, the household is exposed to a heat wave, and the HVAC system is energized. The ability of an HVAC system to maintain the indoor air temperature in its setpoint is dependent on the HVAC maximum cooling capacity, which is a function of the difference between the outdoor air temperature and the temperature setpoint. If the maximum cooling capacity is reached, the indoor air temperature increases from its setpoint (dashed line in Fig 2). This initial deviation does not represent overheating risk unless the caution threshold is reached, as shown in Fig. 2, where residents are exposed to unsafe temperatures. However, if a rotating outage is applied by the power utility, the HVAC de-energization causes a rapid increase in the indoor air temperature due to the lack of cooling capacity to compensate the outdoor temperature effect (solid line in Fig. 2). This fast increase in temperature exposes residents to longer periods with temperatures within the caution hazard level compared to the no-outage case, which at the same time can potentially reach the extreme caution hazard level increasing the risk of heat-related illness.

The exposure duration in the caution and extreme caution hazard levels, shown in Fig. 2, can be extracted to evaluate the overheating risk for the affected household. While the number of hours in the caution and extreme caution hazard levels provides a quantification of the exposure risk, the shaded area among the indoor air temperature during power outage and the caution threshold—or the temperature with no outage if greater—represents the overheating risk resulting from the power outage occurrence, which considers both the duration and temperature rise above the threshold. Notice that this temperature response may not occur in every household, since it depends on the HVAC capacity and its efficiency, showing that some household could be

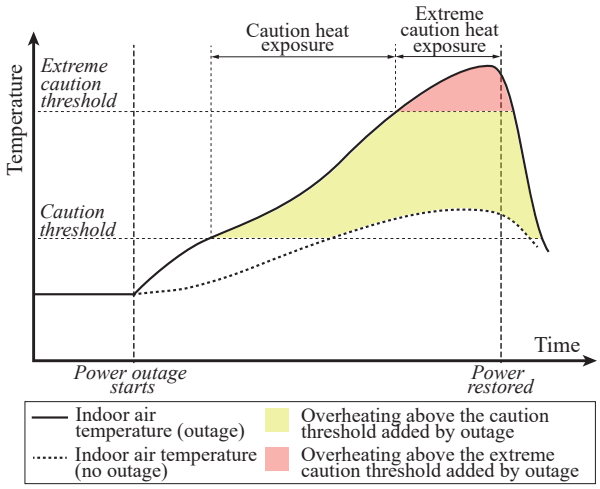

Figure 2. Indoor air temperature during a power outage and related household overheating risk

inequitably more exposed than others if their building envelope has less effective insulation or HVAC system. Hence, the purpose of the proposed framework is to quantify the overheating risk and resulting inequity from the occurrence of power outages during extreme heat waves, which eventually provides a mechanism to guide power distribution system planning.

3. The Proposed Framework

The proposed framework to evaluate overheating risk and inequity during power outages is shown in Fig. 1. In the proposed framework, it is assumed that the loads in power distribution feeders are composed of the aggregation of customers, who reside in single-family houses with pre-defined archetypes. The components of the proposed framework are presented next.

3.1. House Thermal Simulation

In this stage, the indoor air temperature experienced by each customer is determined based on the outdoor air temperature data and the parameters related to the customer's house. The house parameters include thermal resistance and capacitance, which is related to geometry and construction of the building. For the indoor air temperature estimation, it is assumed that each customer's house is equipped with an HVAC system. Since this study is centered on the response to heat waves, only the operation for cooling is considered. The installed HVAC system at customer c house is assumed to have a maximum power consumption $\overline{p_c^{\text{hvac}}}$ and a coefficient of performance COP_c. In this paper, the house is modeled by an equivalent RC circuit

with thermal resistance R_c and thermal capacitance C_c, which can be obtained as given in [16].

During the HVAC cooling operation, the steady-state power required to maintain the indoor air temperature of house c connected to node i at time t at a desired reference temperature, $p^{\text{hvac}}_{c,i,t}$, is calculated as:

$$p^{\text{hvac}}_{c,i,t} = \frac{\theta^{\text{out}}_t - \theta^{\text{ref}}_{c,i,t}}{COP_c R_c}, \quad (1)$$

where θ^{out}_t is the outdoor air temperature at time t, $\theta^{\text{ref}}_{c,i,t}$ is the indoor temperature setpoint for house c at time t. If the required power by the HVAC does not exceed the operation limits of the unit c, $\overline{p^{\text{hvac}}_c}$, then it is assumed that the indoor air temperature reaches the temperature setpoint. When the power exceeds the limits, the variation in the temperature is determined by the indoor air temperature dynamics (2), as a function of the previous indoor temperature, the housethermal parameters, and the input power from the HVAC system fixed to the exceeded limit:

$$\theta^{\text{in}}_{c,i,t} = a_c \theta^{\text{in}}_{c,i,t-1} - b_c COP_c p^{\text{hvac}}_{c,i,t-1} + f_c \theta^{\text{out}}_{t-1}, \quad (2)$$

where $a_c = 1 - \Delta t/R_c C_c$, $b_c = \Delta t/C_c$, and $f_c = \Delta t/R_c C_c$, and Δt is the time step between samples.

3.2. Overheating Risk and Inequity Assessment

This section introduces the metrics that are proposed to evaluate the overheating risk of a community supplied by a power distribution feeder and the inequity experienced due to the heat exposure during outage. The metric evaluation process is depicted in Fig. 3.

Initially, the impact of power outage on the overheating risk is assessed at a household level, based on the properties of each house and its HVAC system. Once the overheating risk is calculated for each house, the household overheating risk is mapped into the power distribution system based on the load composition at each node. This nodal overheating risk index is finally used to determine the location of heat-vulnerable areas in the feeder, as well as the inequity in the heat exposure and vulnerability throughout the circuit.

3.2.1. Household Overheating Risk Assessment: Multiple criteria are found in literature to describe thermal comfort and risk, which consider meteorological variables or heat-budget models [4]. In particular, the index required for this assessment needs to quantify the exposure to high temperatures as well as the duration of the outage itself. The first index is based on the *heat index*, which defines different hazard levels based on the indoor temperature and relative humidity

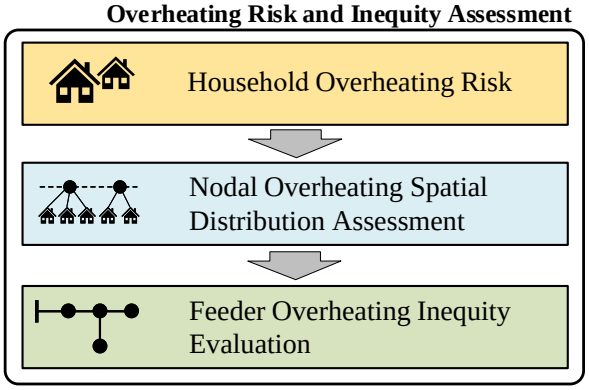

Figure 3. Metrics for the overheating risk and inequity assessment

[12]. Initially, the exposure duration to a hazard level is obtained, which corresponds to the duration in hours where the indoor air temperature falls within the limits of the heat index hazard levels, and it is used to estimate the overall overheating of the household, averaged in the number of days D:

$$u^h_{c,i,x} = \frac{1}{D} \sum_{t \in \mathcal{T}'} f(\min\{\theta_{c,i,t} - \underline{\theta_x}, \overline{\theta_x} - \theta_{c,i,t}\}) \Delta t, \quad (3)$$

where $\mathcal{T}'$ is the subset of time steps where the outage occurs, $\overline{\theta_x}, \underline{\theta_x}$ are the upper and lower thresholds of caution (C) and extreme caution (EC) hazard level $x = \{\text{C,EC}\}$, and $f(z) = 1$ if $z > 0$, $f(z) = 0$ otherwise. The heat index considers four different thresholds for different heat risk categories [17]. In this method, the caution (C) and extreme caution (EC) thresholds, between 27 °C and 32 °C and between 32 °C and 39 °C, respectively, are considered as indoor air temperatures are not expected to reach the danger hazard level. The index, named *weighted unsafe heat hours per household*, combines the unsafe heat exposure duration in the caution and extreme caution levels, assigning weights w_x according to their risk, calculated as:

$$HUH_{c,i} = \sum_{x \in \{\text{C,EC}\}} w_x u^h_{c,i,x}. \quad (4)$$

The second index for household overheating risk is named *overheating risk added by the power outage*, which refers to the degree-hours that are added when the house is subject to a power outage per day, which combines the duration of the disruption with the magnitude of the temperature deviation:

$$v^h_{c,i,x} = \frac{1}{D} \sum_{t \in \mathcal{T}^*} (\theta_{c,i,t} - \max\{\underline{\theta_x}, \theta^o_{c,i,t}\}) y^x_{c,i,t} \Delta t, \quad (5)$$

where $y^x_{c,i,t} = 1$ if $\theta_{c,i,t} \geq \underline{\theta_x}$, and $y^x_{c,i,t} = 0$, otherwise, and $\mathcal{T}^*$ is an evaluation window from the outage occurrence until the temperature lowers to its safe value. The total overheating risk caused by the power outage is obtained from combining the degree-hours calculated for each risk range:

$$AHV_{c,i} = \sum_{x \in \{\text{C,EC}\}} w_x v^h_{c,i,x}. \tag{6}$$

3.2.2. Overheating Spatial Distribution Assessment: Two indicators are used to aggregate the household overheating risk to the nodes the houses are connected to. This aggregation seeks to reflect the concentration of vulnerable households at a given node, as well as the impact of avoiding power de-energization on the aggregated heat vulnerability experienced in the node. The household weighted unsafe heat hours are aggregated to each node as *total number of unsafe heat hours per node*, which corresponds to the summation of weighted unsafe hours of households $c \in \mathcal{C}$ connected to the node i:

$$NUH_i = \sum_{c \in \mathcal{C}} N_{c,i} HUH_{c,i}, \tag{7}$$

where $N_{c,i}$ is the number of households with archetype c connected to node i. This metric is linked to the concentration of households and displays higher values for nodes with a higher number of households. On the other hand, the household-level added overheating risk by the power outage is aggregated at each node as *overheating risk sensitivity to power outages*, which quantifies the benefit of sustained energization of a node during a rotating outage, and is calculated as the ratio of the total overheating risk caused by the outage $AHV_{c,i}$ and the total energy curtailed during the power outage:

$$OAE_i = \frac{\sum_{c \in \mathcal{C}} N_{c,i} AHV_{c,i}}{\sum_{t \in \mathcal{T}'} p^l_{i,t} \Delta t}, \tag{8}$$

where $p^l_{i,t}$ is the load of node i at time t. The value of this index is higher when the total overheating risk caused by the outage is large compared to the amount of energy curtailed at the node.

3.2.3. Feeder-level Overheating Inequity Assessment: The overall overheating risk inequity that is perceived at the feeder is calculated as a function of the nodal equivalent risk of overheating. A feeder-level metric, named *Overheating Risk Inequity Score (ORIS)*, quantifies the range from where the nodal equivalent risk of overheating metric varies for a given operation scenario:

$$ORIS = \overline{OAE} - \underline{OAE}, \tag{9}$$

where $\overline{OAE}$ and $\underline{OAE}$ and the maximum and minimum nodal equivalent risk of overheating metric. Higher values of this metric indicates a greater disparity in the overheating risk aggregated between nodes. Smaller values of the ORIS metric represent a more equitable operational scenario.

3.3. Sensitivity Assessment

In this step, a model to assess the performance of a power distribution system to mitigate the overheating risk given a configuration of DERs and automated switches is formulated. This assessment seeks to dispatch the available resources—DERs and power procured from the bulk transmission system—to avoid de-energization that leads households connected to the node to experience overheating. Each customer profile corresponds to the combination of the base non-cooling load $p^{l,\text{fx}}_{i,t}$ plus the power consumption from the HVAC system. The total load at each node of the distribution system consists of a composition of different house archetypes, given the location and socio-demographic attributes of the customers supplied:

$$p^l_{i,t} = p^{l,\text{fx}}_{i,t} + \sum_{c \in \mathcal{C}} N_{c,i} p^{\text{hvac}}_{c,i,t}, \tag{10}$$

where $p^l_{i,t}$ is the total load at node i, time t, and $p^{l,\text{fx}}_{i,t}$ is the non-cooling load component. The power grid assessment is implemented through the optimization model (11)–(26) which minimizes the cost of the energy procured from the bulk transmission system, by dispatching DERs and defining the automation switch position, subject to balance constraints and operation limits for voltages:

$$\min \sum_{t \in \mathcal{T}} \left(\lambda^{\text{grid}}_t p^{\text{grid}}_t + \sum_{i \in \mathcal{B}} \left(\lambda^{\text{dg}}_{i,t} p^g_{i,t} + (1 - e_{i,t}) OAE_i \right) \right) \Delta t, \tag{11}$$

s.t.

$$p^g_{i,t} + p^d_{i,t} - p^c_{i,t} - p^l_{i,t} e_{i,t} = \sum_{j|i \to j} p_{ij,t} - \sum_{j|j \to i} p_{ji,t}, \tag{12}$$

$$q^g_{i,t} + q^e_{i,t} - q^l_{i,t} e_{i,t} = \sum_{j|i \to j} q_{ij,t} - \sum_{j|j \to i} q_{ji,t}, \tag{13}$$

$$v_{j,t} \leq v_{i,t} - 2(r_{ij} p_{ij,t} + x_{ij} q_{ij,t}) + M(1 - s_{ij,t}), \tag{14}$$

$$v_{j,t} \geq v_{i,t} - 2(r_{ij}p_{ij,t} + x_{ij}q_{ij,t}) - M(1 - s_{ij,t}), \quad (15)$$

$$\underline{v_i} \leq v_{i,t} \leq \overline{v_i}, \quad (16)$$

$$|s_{ij,t} - s_{ij}^d| \leq b_{ij}, \quad t = 1, \quad (17)$$

$$|s_{ij,t} - s_{ij,t-1}| \leq b_{ij}, \quad t > 1, \quad (18)$$

$$|e_{i,t} - e_{j,t}| \leq 1 - s_{ij,t}, \quad (19)$$

$$-\overline{p_{ij}} s_{ij,t} \leq p_{ij,t} \leq \overline{p_{ij}} s_{ij,t}, \quad (20)$$

$$-\overline{q_{ij}} s_{ij,t} \leq q_{ij,t} \leq \overline{q_{ij}} s_{ij,t}, \quad (21)$$

$$0 \leq p_{i,t}^g \leq \overline{p_i^g}, \quad (22)$$

$$-\overline{q_{i,t}^g} \leq q_{i,t}^g \leq \overline{q_{i,t}^g}, \quad (23)$$

$$E_{i,t} = E_{i,t-1} + \left(\eta_i^c p_{i,t}^c - p_{i,t}^d / \eta_i^d\right) \Delta t, \quad (24)$$

$$0 \leq p_{i,t}^d, p_{i,t}^c \leq \overline{p_i^e}, \quad (25)$$

$$\underline{E_i} \leq E_{i,t} \leq \overline{E_i}. \quad (26)$$

For modeling purposes, it is considered that each line ij contains a switch whose operation can be enabled by the binary parameter b_{ij}. The objective function (11) minimizes the cost of energy transactions with the bulk transmission system and DERs, along with overheating risk resulting from the node de-energization (given by metric OAE_i), where p_t^{grid} is the power procured from the bulk transmission system at time t at unit price λ_t^{grid}, $p_{i,t}^g$ is the power procured from the distributed generator i at time t with unit price $\lambda_{i,t}^{\text{dg}}$, and $e_{i,t}$ is the energization status of node i at time i. The active and reactive power balance are formulated in (12)–(13), where $p_{i,t}^d, p_{i,t}^c$ are respectively the discharging and charging power from the energy storage (ES) system installed at node i during time t, $p_{i,t}^l, q_{i,t}^l$ are the total active and reactive load connected to node i at time t, respectively, $p_{ij,t}, q_{ij,t}$ is the active and reactive power flow from node i to node j at time t, and $q_{i,t}^g, q_{i,t}^e$ is the reactive power generated by the distributed generator and ES system connected at node i, time t. The voltage drop is formulated in (14)–(15) for each line section to decouple the voltages at each end if the line is open, where $v_{i,t}$ is the squared voltage at node i, time t, r_{ij}, x_{ij} are the resistance and reactance of line ij, $s_{ij,t}$ is the status of the switch installed at line ij at time t, and M is a large number. The voltage limits are given by (16). The switching operation is enabled by (17)–(18), where s_{ij}^d is the default switch position at the beginning of the time horizon, and b_{ij} is a binary parameter equals to 1 if a switch is installed at line ij, and 0 otherwise. The energization of nodes connected through a line is coupled by (19), where the energization status of two nodes must be the same if the switch connecting both nodes is open (if no switch is installed, the connection through a line is considered a closed switch unable to trip). The maximum active and reactive power flows in lines are limited in (20)–(21), which is subject to the switch status. The distributed generation limits are given in (22)–(23), where $\overline{p_i^g}, \overline{q_i^g}$ are the maximum active and reactive power outputs from the distributed generation at node i. The changes in the state of charge of the ES systems is calculated according to (24), where $E_{i,t}$ is the state of charge of the ES systems connected to node i at time t, and η_i^c, η_i^d are the charging and discharging efficiencies. The charging and discharging power are limited as given by (25) with $\overline{p_i^e}$ is the maximum power output from the ES system i. Finally, the state of charge is limited to its upper and lower limits $\overline{E}_i, \underline{E}_i$ in (26).

4. Case Study

The proposed framework to assess the community overheating risk and the impact of the heat wave on the power distribution system operation is tested on the IEEE 33-node test system shown in Fig. 4-a. In this test system, loads represent aggregations of customers, where load profiles consider the customers' HVAC and non-cooling power consumption. Four archetypes are considered with different combinations of insulation features—modeled by the thermal resistance and capacitance as an RC circuit—and different efficiencies for the cooling process, represented by parameters shown in Table 1 [18]. The indoor air temperature and power consumption calculation during a heat wave is done by considering the hourly outdoor air temperature of San Joaquin Valley measured at Fresno State Station from August 14th, 2020 at 00:00 h to August 16th, 2020 at 00:00 h, considering a 49 hour long window from a heat wave scenario [19], shown in Fig. 4-b. The locational marginal prices for the area, required for the electricity cost calculations, are obtained from California Independent System Operator for the indicated periods [20]. The reference temperature is assumed to be fixed at 25 °C, and the caution and extreme threshold are respectively set as 27°C and 32°C according to [17].

Table 1. House Archetype Parameters

Archetype	1	2	3	4
Thermal resist. (kWh/°C)	1.75	2.25	2.75	3.25
Thermal capac. (°C/kW)	1.75	2.0	2.25	3.0
Coef. of performance	1.7	1.7	2.5	2.5
Max. power input (kW)	4.0	4.0	4.0	4.0

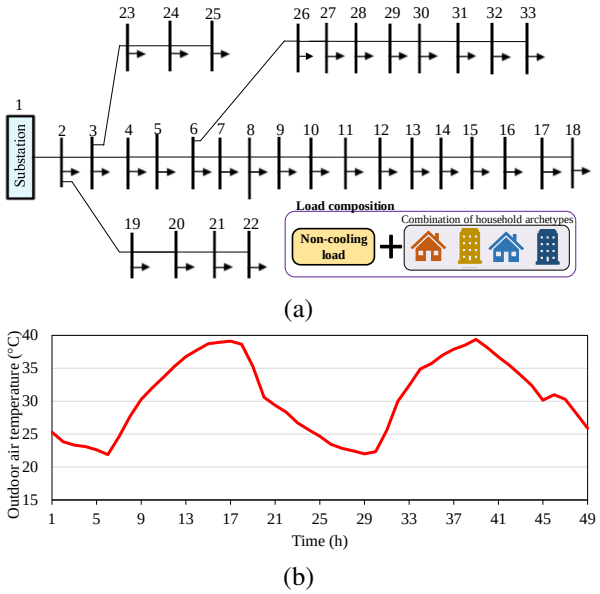

Figure 4. (a) IEEE 33-node test system for framework evaluation (b) Outdoor air temperature for heat wave scenario

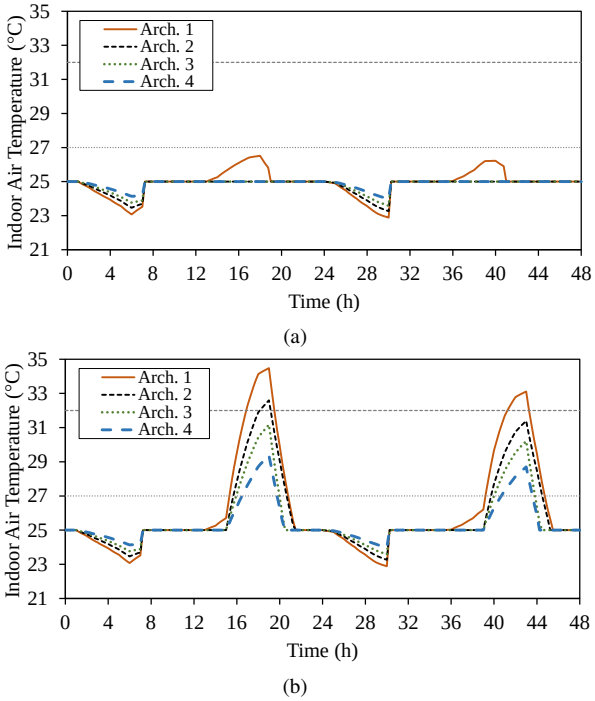

Figure 5. Indoor air temperature during heat wave (a) no power outage (b) under power outage

4.1. Effect of the Power Outage on Household-level Overheating Risk

To assess the impact of the power outage on the household overheating risk during a heat wave, the indoor air temperature and associated overheating risk metrics for each household are calculated when subject to a four-hour long power outage. Initially, the indoor air temperature during the heat wave with no power outage is displayed in Fig. 5-a.

The temperature drops observed in Fig. 5-a correspond to nighttime period, where the outdoor air temperature is below the reference temperature, disabling the HVAC system operation. In this scenario, only the indoor temperature of households with archetype 1 shows a deviation from the temperature setpoint caused by the combined low coefficient of performance and maximum capacity of the installed HVAC system. However, the maximum temperature value reached in this scenario remains below the caution hazard level, representing a safe condition for the household. In case of power outage, the temperature response for each archetype is shown in Fig. 5-b. In this scenario, archetypes 1 to 4 experience a deviation from the setpoint temperature caused by the HVAC malfunction during the power outage. However, the temperature rise differs among archetypes due to the differences in building envelope properties. Archetype 1, which has a lower thermal time constant, experiences the fastest temperature rise, followed by archetypes 2, 3, and 4 that successively have greater time constants. The temperature deviation exposes residents of each house archetype to unsafe heat exposure in the caution and extreme caution hazard levels with different durations. The average exposure duration of each archetype in each of the considered heat risk categories during the two-day horizon is summarized in Fig. 6. In Fig. 6, archetype 1 experiences risk for almost the complete duration of the power outage and mainly in the extreme caution hazard level. The exposure to the extreme caution hazard level is less for archetype 2 as it is only experienced for one day, and during no hours for archetypes 3 and 4, which remain in the caution hazard level.

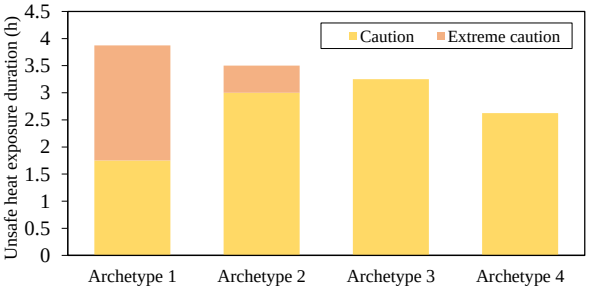

Figure 6. Hours of exposure to caution and extreme caution temperatures per archetype

4.2. Effect of the Power Outage Duration on the Overheating Risk

The overheating risk experienced at each house is dependent on the outage duration. The results of NUH and AHV metrics for different outage durations in steps of 15 min are displayed in Fig. 7-(a) and 7-(b), respectively. Figure 7 shows that archetypes may not experience any overheating risk until several time periods after the power outage starts. As expected, archetype 1 is affected sooner and the metric values increase faster compared to archetypes 2 to 4. As the results obtained for each hazard level are weighted differently, the metric evolution displays a non-linear growth associated with the unsafe heat hours during the extreme caution hazard, which represents the higher risk related to the exposure to temperatures in this range.

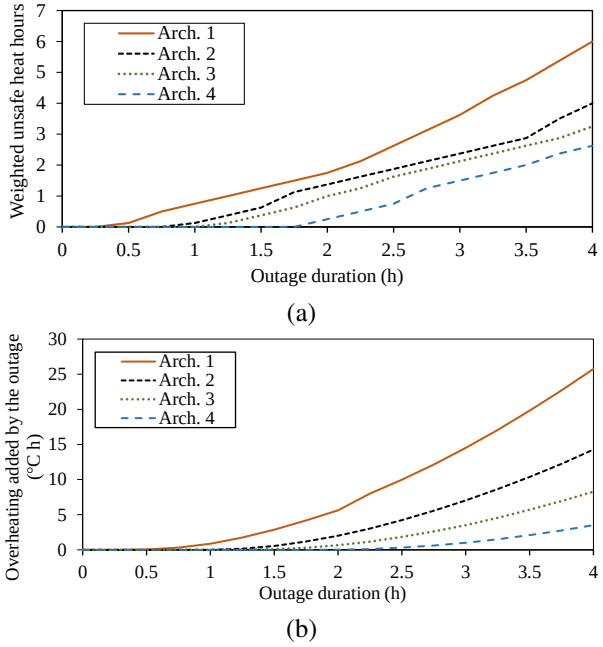

Figure 7. Household overheating risk metrics as a function of outage duration: (a) Weighted unsafe heat hours, (b) Overheating risk added by the power outage

4.3. Nodal-level Overheating Spatial Distribution Assessment

The household-level metrics obtained for the four-hour long outage scenario are aggregated at a nodal level and displayed in Fig. 8. Two different aspects are highlighted by the nodal-level vulnerability aggregation. Metric NUH displays higher values in presence of a higher concentration of households and intensified

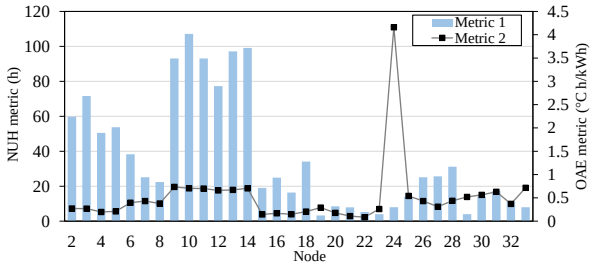

Figure 8. Nodal metrics for spatial vulnerability distribution assessment

under the presence of highly vulnerable households. On the other hand, metric OAE assigns higher values to the nodes where overheating risk is high compared to the demand being supplied at the node. In this case, node 24 has a lower demand but a higher concentration of vulnerable households, displaying a considerable higher value. Following node 24, the value of the metric is also significant for the group of nodes 9 to 14, indicating that in addition to a higher number of households being supplied from these nodes, there is also a high presence of overheating risk that can be reduced if the outage duration is reduced for these nodes. In general, metric OAE satisfactorily displays higher values in nodes with a larger number of highly vulnerable households, and can potentially guide a planning process towards an equitable planning process.

4.4. Sensitivity Assessment to Distributed Energy Resource Inclusion

In this section, the effect of power distribution system investments on the overheating risk and inequity is assessed. Investments include installation of distributed energy resources and switches for isolation is assessed. Based on Fig. 8, nodes with a higher nodal OAE, which correspond to nodes where the aggregation of customers contains a majority of households with archetype 1, are selected to be isolated with switches and partially energized with distributed energy resources installed in the resulting island.

From the evaluation of the metric OAE in Fig. 8, three high risk regions are identified. Let us assume that switches can be added to lines 23-24, 27-28, 30-31, 8-9, and 14-15 to isolate the high vulnerable nodes, and that DERs with sufficient capacity are installed to sustain the operation within the section for a specific period. Section 1 contains nodes 9 to 14, section 2 contains nodes 24 and 25, and section 3 contains nodes 28-30. The resulting designs to sustain the power supply in the section for one hour (case 1), two hours (case 2), and three hours (case 3) are shown in Table 2.

Table 2. Distributed energy resource designs for overheating mitigation

Cases		Sec. 1	Sec. 2	Sec. 3
Case 1	Solar out. (kW)	250	10	35
	Batt. out. (kW)	1250	50	175
	Batt. cap. (kWh)	1250	50	175
Case 2	Solar out. (kW)	500	20	70
	Batt. out. (kW)	1250	50	175
	Batt. cap. (kWh)	2500	100	350
Case 3	Solar out. (kW)	750	30	105
	Batt. out. (kW)	1250	50	175
	Batt. cap. (kWh)	3750	150	525

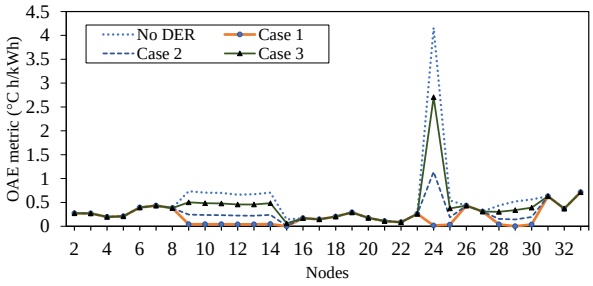

Figure 9. Nodal overheating risk under different DER installations

The resulting OAE for all nodes in each of the proposed cases is depicted in Fig. 9. In all cases, the addition of distributed energy resources to the high-vulnerable sections reduces the aggregated overheating risk at each node. Notice that, given the non-linear nature of the overheating risk with the outage duration, the benefit of de-energizing three hours instead of four is more significant than the benefit of de-energizing two hours instead of three. The impact of these DER installations on the perceived heat inequity in the distribution system is quantified by the ORIS index, which is summarized in Table 3.

Table 3. Evaluating overheating risk inequity for different DER installations

	No DER	Case 1	Case 2	Case 3
ORIS	4.075	2.643	1.132	0.715

The ORIS index quantifies the disparity in the overheating risk distribution among the nodes in the power distribution system. By adding energy resources, the trend is to reduce also the existing gap among the maximum and minimum value of metric OAE of the feeder nodes. The non-linear nature of the metrics leads to higher reductions in the overheating risk between the base case and cases 1 and 2; However, notice that in Case 3, the reduction is less and the metric indicates that other nodes should be prioritized, for example node 31 and 33, which become the nodes with the higher OAE metric instead of the nodes in the initial defined sections. This result suggests that the resource distribution can be achieved by defining an appropriate heuristic method or through mathematical optimization.

5. Conclusion

Power grids and communities worldwide are experiencing the increasing impact of extreme weather events caused by climate change. This paper developed a framework to assess the impact of power outages on the resilience of power distribution systems during a heat wave and the risk of overheating for the communities affected by extreme heat. The proposed framework quantifies the overheating risk based on the house attributes, including insulation, HVAC efficiency, and capacity. Starting from a household overheating analysis, the household overheating risk is mapped into the power distribution system to identify the most heat-vulnerable areas during blackouts and quantify the overall inequity in overheating risk exposure. The results demonstrate that the framework identifies nodes with a concentration of households with high overheating risk and provides insights on where to take action to reach a more equitable operational condition for the feeder. This framework also provides a tool for power utility companies as the metrics inform the power outage impact on the community, which can used as an input when defining operational strategies such as rotating outages. In addition, the metrics provide insights on how to support planning towards mitigating inequity, which should focus on isolating through automation and providing enough capacity in the feeder section to avoid long power supply interruptions for the most vulnerable consumers.

References

[1] Q. Schiermeier. “Climate change made north america’s deadly heatwave 150 times more likely.” (Jul. 2021), [Online]. Available: `https://www.nature.com/articles/d41586-021-01869-0`.

[2] California Independent System Operator, California Public Utilities Commission, and California Energy Commission, “Final Root Cause Analysis: Mid-August 2020 Extreme Heat Wave,” Tech. Rep., 2021.

[3] S. Meerow and L. Keith, “Planning for extreme heat,” *Journal of the American Planning Association*, vol. 88, no. 3, pp. 319–334, 2022.

[4] K. Sun, W. Zhang, Z. Zeng, R. Levinson, M. Wei, and T. Hong, "Passive cooling designs to improve heat resilience of homes in underserved and vulnerable communities," *Energy and Buildings*, vol. 252, p. 111 383, 2021, ISSN: 0378-7788.

[5] H. T. Nguyen, J. Muhs, and M. Parvania, "Preparatory operation of automated distribution systems for resilience enhancement of critical loads," *IEEE Transactions on Power Delivery*, vol. 36, no. 4, pp. 2354–2362, 2021. DOI: 10.1109/TPWRD.2020.3030927.

[6] H. T. Nguyen, J. W. Muhs, and M. Parvania, "Assessing impacts of energy storage on resilience of distribution systems against hurricanes," *Journal of Modern Power Systems and Clean Energy*, vol. 7, no. 4, pp. 731–740, 2019.

[7] M. M. Hosseini and M. Parvania, "Quantifying impacts of automation on resilience of distribution systems," *IET Smart Grid*, vol. 3, no. 2, pp. 144–152, 2020. DOI: https://doi.org/10.1049/iet-stg.2019.0175.

[8] L. Rodriguez-Garcia, M. M. Hosseini, T. M. Mosier, and M. Parvania, "Resilience analytics for interdependent power and water distribution systems," *IEEE Transactions on Power Systems*, vol. 37, no. 6, pp. 4244–4257, 2022.

[9] S. Attia, R. Levinson, E. Ndongo, *et al.*, "Resilient cooling of buildings to protect against heat waves and power outages: Key concepts and definition," *Energy and Buildings*, vol. 239, p. 110 869, 2021, ISSN: 0378-7788.

[10] R. Rahif, D. Amaripadath, and S. Attia, "Review on time-integrated overheating evaluation methods for residential buildings in temperate climates of europe," *Energy and Buildings*, vol. 252, p. 111 463, 2021, ISSN: 0378-7788. [Online]. Available: https://www.sciencedirect.com/science/article/pii/S0378778821007477.

[11] Z. Wang, T. Hong, and H. Li, "Informing the planning of rotating power outages in heat waves through data analytics of connected smart thermostats for residential buildings," *Environmental Research Letters*, vol. 16, no. 7, p. 074 003, Jun. 2021.

[12] M. Sheng, M. Reiner, K. Sun, and T. Hong, "Assessing thermal resilience of an assisted living facility during heat waves and cold snaps with power outages," *Building and Environment*, vol. 230, p. 110 001, 2023, ISSN: 0360-1323.

[13] Z. Zeng, W. Zhang, K. Sun, M. Wei, and T. Hong, "Investigation of pre-cooling as a recommended measure to improve residential buildings' thermal resilience during heat waves," *Building and Environment*, vol. 210, p. 108 694, 2022, ISSN: 0360-1323.

[14] California Public Utilities Commission. "Disadvantaged communities." (2021), [Online]. Available: https://www.cpuc.ca.gov/industries-and-topics/electrical-energy/infrastructure/disadvantaged-communities.

[15] National Institute for Occupational Safety and Health. "Heat stress – heat related illness." (2022), [Online]. Available: https://www.cdc.gov/niosh/topics/heatstress/heatrelillness.html.

[16] G. Chen, H. Zhang, H. Hui, N. Dai, and Y. Song, "Scheduling thermostatically controlled loads to provide regulation capacity based on a learning-based optimal power flow model," *IEEE Transactions on Sustainable Energy*, vol. 12, no. 4, pp. 2459–2470, 2021.

[17] National Oceanic and Atmospheric Administration. "Heat forecast index." (), [Online]. Available: https://www.weather.gov/safety/heat-index.

[18] H. Hao, B. M. Sanandaji, K. Poolla, and T. L. Vincent, "Aggregate flexibility of thermostatically controlled loads," *IEEE Transactions on Power Systems*, vol. 30, no. 1, pp. 189–198, 2015.

[19] California Irrigation Management Information System (CIMIS). (2023), [Online]. Available: https://cimis.water.ca.gov/.

[20] California ISO Open Access Same-time Information System (OASIS). (2023), [Online]. Available: http://oasis.caiso.com/.